From E_{2g} to Other Modes: Effects of Pressure on Electron-Phonon Interaction in MgB_2

Prabhakar P. Singh*

Department of Physics, Indian Institute of Technology, Powai, Mumbai- 400076, India

(Received 27 August 2006; published 14 December 2006)

We study the effects of pressure on the electron-phonon interaction in MgB_2 using density-functional-based methods. Our results show that the superconductivity in MgB_2 vanishes by 100 GPa, and then *reappears* at higher pressures. In particular, we find a superconducting transition temperature $T_c \approx 2$ K for $\mu^* = 0.1$ at a pressure of 137 GPa.

DOI: 10.1103/PhysRevLett.97.247002 PACS numbers: 74.70.Ad, 74.25.Jb, 74.25.Kc

The superconductivity in MgB_2 [1] is intimately connected with the holes in the B $p_{x(y)}$ and p_z bands [2–4] and their coupling to the in-plane E_{2g} phonon mode [5–8]. Several experiments on MgB_2 under pressure [9–11] show a reduction in superconducting transition temperature T_c at a rate of $-1.1\ \mathrm{K\,GPa^{-1}}$, which can be understood in terms of a continuous weakening of E_{2g} phonon mode coupling. Based on this picture, it is estimated that the superconductivity in MgB_2 will vanish by 90–100 GPa [12].

Recent experiments on elemental Li [13,14] and Y [15] have shown a significant increase in their T_c with an increase in pressure. For example, the T_c of Y changes from 6 mK [16] to 20 K [15] as the pressure is increased from ambient to 115 GPa. In light of these experiments, it would be interesting to see what happens to the superconducting properties, especially T_c, of MgB_2 beyond 90–100 GPa.

In this Letter, we report on our density-functional-based study of the evolution of electron-phonon interaction in MgB_2 as a function of pressure up to 150 GPa. Additionally, we have solved the isotropic Eliashberg gap equation to obtain T_c of MgB_2 as a function of pressure.

Based on our calculations, we find that the increase in pressure hardens the MgB_2 lattice and dramatically reduces the contribution of the E_{2g} phonon mode to the electron-phonon coupling. As a result, the superconductivity in MgB_2 vanishes by 100 GPa, only to *reappear* at higher pressures. In particular, we find a superconducting transition temperature $T_c \approx 2$ K for $\mu^* = 0.1$ at a pressure of 137 GPa. We also find that the B_{1g} phonon mode completely softens around A symmetry point by 143 GPa. Before we describe our results, we briefly outline the computational details of our calculations.

We have calculated the electronic structure and the electron-phonon interaction of MgB_2 in $P6/mmm$ crystal structure as a function of pressure up to 150 GPa. The lattice constants a and c for different pressures were taken from Ref. [12], which agree well in the range of pressures where experiments have been reported. The electronic structure was calculated using the full-potential linear muffin-tin orbital (LMTO) method [17,18] as well as the plane-wave pseudopotential method using PWSCF package [19]. The phonon dispersion $\omega_{\mathbf{q}\nu}$, the phonon linewidth $\gamma_{\mathbf{q}\nu}$, the phonon density of states $F(\omega)$, and the Eliashberg function $\alpha^2F(\omega)$, were calculated using the density-functional perturbation theory [20] as implemented in the PWSCF package. Finally, the isotropic Eliashberg gap equation [21–23] has been solved for a range of μ^* to obtain the corresponding T_c.

The charge self-consistent, full-potential, LMTO calculations for MgB_2 were carried out using the local-density approximation for exchange correlation of Perdew *et al.* [24], 3κ-energy panels, and 793 $\mathbf{k}$ points in the irreducible wedge of the Brillouin zone (BZ). The $2p$ state of Mg was treated as a semicore state. The basis set used consisted of s, p, and d orbitals at the Mg and the B sites, and the potential and the wave function were expanded up to $l_{\max} = 6$. The muffin-tin spheres for Mg and B were taken to be slightly smaller than the touching spheres in each case. These calculations are used to study the symmetry-resolved densities of states as well as the band structure along the high symmetry directions in the corresponding BZ.

For calculating the Fermi surface, the phonon dispersion, the phonon density of states, and the Eliashberg function, we have used the plane-wave pseudopotential method with Vanderbilt's ultrasoft pseudopotentials with nonlinear core correction. The kinetic energy cutoff for the wave function was 35 Ry, and for the charge density and the potential it was 200 Ry. The exchange-correlation potential was parametrized as suggested by Perdew *et al.* [24]. The Fermi surface was constructed using eigenvalues calculated on a $36 \times 36 \times 36$ grid in the reciprocal space. The linear-response calculations were carried out on a $6 \times 6 \times 6$ grid resulting in 28 irreducible $\mathbf{q}$ points. A $12 \times 12 \times 12$ grid of $\mathbf{k}$ points is used for the BZ integrations during linear-response calculations. The electron-phonon matrix elements are sampled more accurately on a $36 \times 36 \times 36$ grid using the double-grid technique. To check the convergence of our linear-response calculations, we have used an $18 \times 18 \times 18$ and $24 \times 24 \times 24$ grids for carrying out the BZ integrations during self-consistency for points along Γ-A direction as well as for pressures above

125 GPa. The convergence of electron-phonon matrix elements were checked with grids up to $40 \times 40 \times 40$ in the reciprocal space.

The B $p_{x(y)}$ and p_z densities of states (DOS) play a crucial role in determining the superconducting properties of MgB_2. Our calculated B $p_{x(y)}$ and p_z DOS as a function of pressure are shown in Fig. 1, where we also show the DOS in a 10 mRy energy window around Fermi energy E_F in a separate panel. With increasing pressure both $p_{x(y)}$ and p_z DOS flatten and the states are pushed further down. Because with increasing pressure the lattice constant c decreases much more rapidly than a in MgB_2, as a result the $p_{x(y)}$ DOS around E_F is significantly reduced. Between 100 and 137 GPa the $p_{x(y)}$ DOS is inside E_F with essentially no holes. However, the p_z DOS around E_F is in tact up to 137 GPa. Such a situation is very different from the usual band filling that takes place when we put Al and/or C as impurities in MgB_2. These differences can be further highlighted by considering the changes in the band structure along high symmetry directions in the BZ of MgB_2 as a function of pressure.

In Fig. 2, we show the calculated band structure of MgB_2 along high symmetry directions in the Brillouin zone. The states along Γ-A have B $p_{x(y)}$ character while states at M are of B p_z type. With increasing pressure, as can be seen from Fig. 2, the states along Γ-A move toward E_F while the states at M move away from E_F. By 137 GPa, all the B $p_{x(y)}$-derived states along Γ-A are close to being inside E_F, while the states at M have moved up by almost 0.17 Ry. The movement of states along Γ-A and M with an increase in pressure, in conjunction with doping of MgB_2, can be more effective in tuning its superconducting properties.

A complete picture of the pressure-induced changes in the electronic structure of MgB_2 emerges through the changes in the Fermi surface, as shown in Fig. 3. We find that the characteristic two-dimensional cylindrical sheets along Γ-A become narrower and constricted around the Γ point with an increase in pressure. With a further increase in pressure, say by 100 GPa, the states manage to form only a small portion of the tube around the A point of the Γ-A direction. The circular opening of the p_z-derived Fermi surface sheets containing (K, M) and (H, L) symmetry points narrows as the band moves up. At a pressure of 137 GPa, the Fermi surface consists of essentially these sheets with the cylindrical tube reduced to a dot around A point. Thus, as long as the states on the cylindrical sheets play a pivotal role in sustaining superconductivity in MgB_2, their absence beyond 100 GPa, as shown in Fig. 3, ensures the vanishing of superconductivity in MgB_2 around 100 GPa and above. Unless, of course, with pressures above 100 GPa the electron-phonon coupling provided by the remaining states is strong enough to *restart* the superconductivity in MgB_2.

To be able to go beyond the qualitative assessments that we have made so far about the pressure-induced changes in the electron-phonon interaction in MgB_2 using the changes in the electronic structure as the backdrop, we have calculated the phonon dispersion, the phonon linewidth, the phonon density of states, and the electron-phonon interaction as a function of pressure up to 150 GPa. We find that in MgB_2 at zero pressure the frequency associated with E_{2g} phonon mode at Γ is 67 meV, which goes up to 148 meV at 137 GPa. Similarly, the frequency of the E_{2u} phonon mode at A point increases from 60 meV at zero pressure to 139 meV at 137 GPa. In contrast, the frequency of the

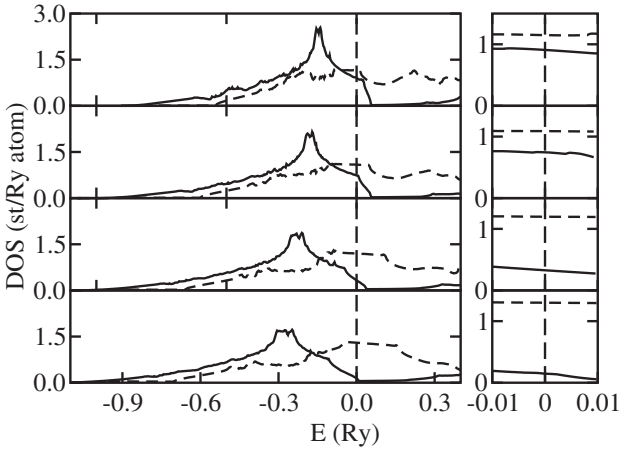

FIG. 1. The B $p_{x(y)}$ (solid line) and the p_z (dashed line) densities of states in MgB_2 as a function of pressure for 0 (1st panel from the top), 50 (2nd panel), 100 (3rd panel), and 137 (4th panel) GPa. The panels on the right show the corresponding densities of states in a 10 mRy energy window around the Fermi energy, which is shown as the vertical, long-dashed line in the figure.

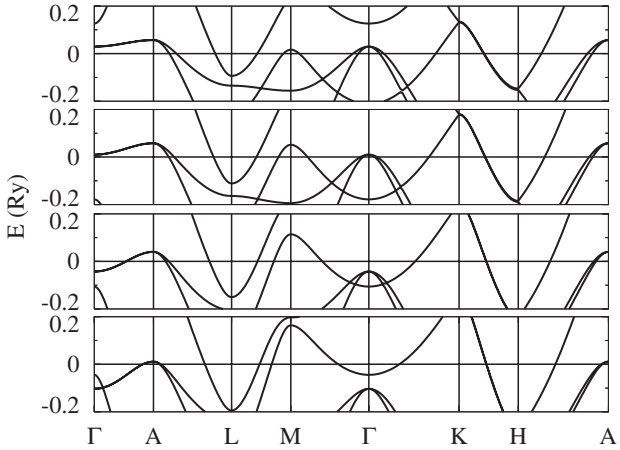

FIG. 2. The band structure of MgB_2 along high symmetry directions in the Brillouin zone as a function of pressure for 0 (1st panel from the top), 50 (2nd panel), 100 (3rd panel), and 137 (4th panel) GPa. The horizontal line, passing through the energy zero, indicates the Fermi energy. Note that the numerical values of the wave vector **k** corresponding to the various symmetry points, as shown in the figure, are different at different pressures.

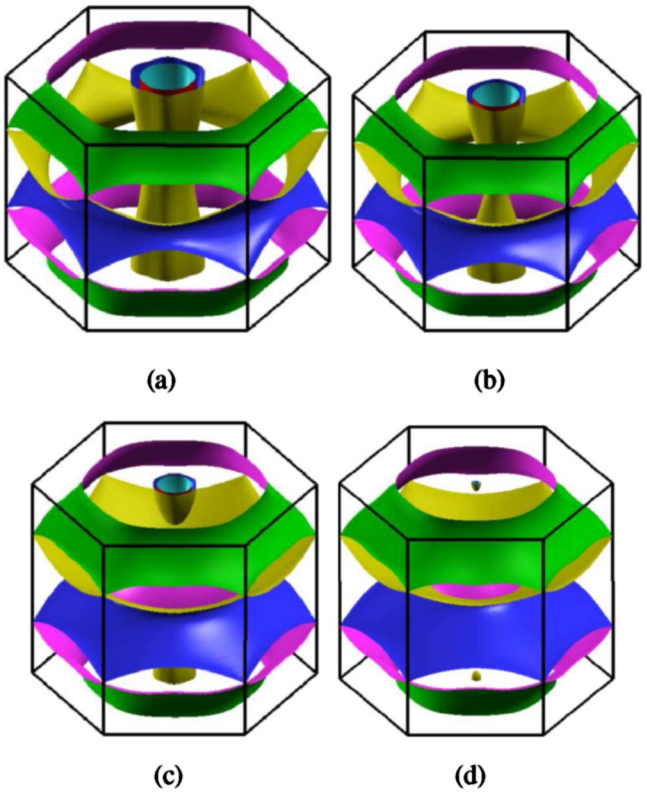

FIG. 3 (color online). The Fermi surface of MgB_2 as a function of pressure in the corresponding Brillouin zone for (a) 0, (b) 50, (c) 100, and (d) 137 GPa, calculated as described in the text.

B_{1g} phonon mode at A point, involving out-of-plane motion of B atoms, reduces from 63 meV at 100 GPa to 34 meV at 125 GPa. As shown in Fig. 4, the softening of B_{1g} mode around A point continues with further increase in pressure and by 143 GPa it has become unstable. The softening of B_{1g} mode around A point is accompanied by an enhanced $\gamma_{\mathbf{q}\nu}$, as can be seen from Fig. 4. Note, however, that the dynamical instability of B_{1g} mode in the present calculation does not necessarily imply a physical instability of the lattice. Under these conditions, the anharmonic effects become important.

Our calculated $F(\omega)$ and $\alpha^2F(\omega)$ of MgB_2 for pressures up to 137 GPa are shown in Fig. 5. For MgB_2 at zero pressure, our results for $F(\omega)$ compare well with previous calculations [5–8]. The decrease in the strength of the electron-phonon coupling in MgB_2 with an increase in pressure can be clearly seen in Fig. 5. The average electron-phonon coupling constant λ, shown in Fig. 6, decreases from 0.68 to 0.28 as the pressure is increased from zero to 100 GPa, which is consistent with the expected loss of superconductivity in MgB_2 by this pressure. By 100 GPa the partial $\lambda_{q\nu}$ of the E_{2g} phonon mode at Γ and A points are reduced by a factor of 3 and 20, respectively. However, the increase in λ to 0.38 by 137 GPa with the possibility of higher values with further increase in pressure, as shown in Fig. 6, suggests the reemergence of superconductivity in MgB_2 at higher pressures *without* the dominance of E_{2g} mode.

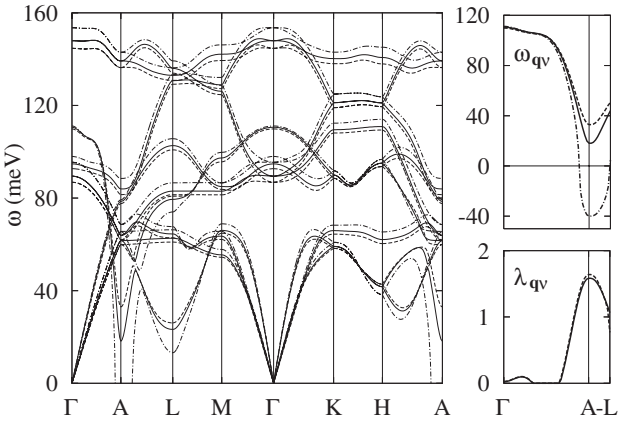

FIG. 4. The phonon dispersion ω of MgB_2 along high symmetry directions in the Brillouin zone (left panel), and the $\omega_{\mathbf{q}\nu}$ (top-right panel) and the $\gamma_{\mathbf{q}\nu}$ (bottom-right panel) for B_{1g} phonon mode along Γ-A-L, as a function of pressure for 125 (dashed line), 137 (solid line) and 143 (dot-dashed line) GPa. The $\omega_{\mathbf{q}\nu}$ and the $\gamma_{\mathbf{q}\nu}$ are in meV, the frequencies below zero (in the top-right panel) are imaginary, and for 143 GPa the $\gamma_{\mathbf{q}\nu}$ is not shown. Note that the numerical values of $\mathbf{q}$ corresponding to the various symmetry points are different at different pressures.

Finally, the change in T_c with pressure has been obtained by solving the isotropic gap equation [22,23] using the calculated Eliashberg function $\alpha^2F(\omega)$ at each pressure. The results of these calculations are shown in Fig. 6 for a range of μ^*. Our results, shown in Fig. 6, predict the

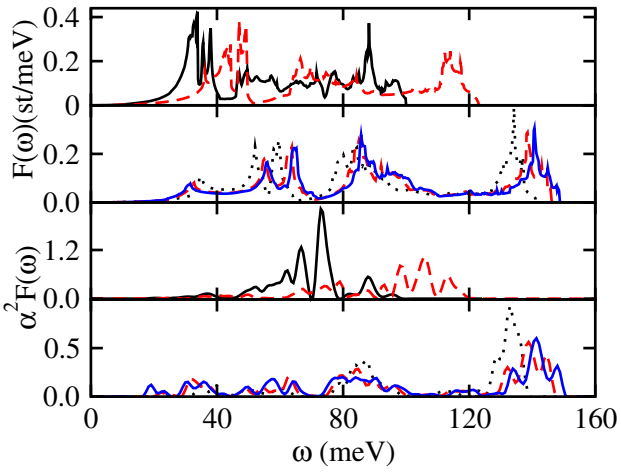

FIG. 5 (color online). The phonon density of states $F(\omega)$ (top 2 panels) and the Eliashberg function $\alpha^2F(\omega)$ (bottom 2 panels) of MgB_2 as a function of pressure. The $F(\omega)$ and $\alpha^2F(\omega)$ for 0 (solid line) and 50 (dashed line) GPa are shown in the 1st panel and the 3rd panel, respectively. The $F(\omega)$ and $\alpha^2F(\omega)$ for 100 (dotted line), 125 (dashed line), and 137 (solid line) GPa are shown in the 2nd panel and the 4th panel, respectively.

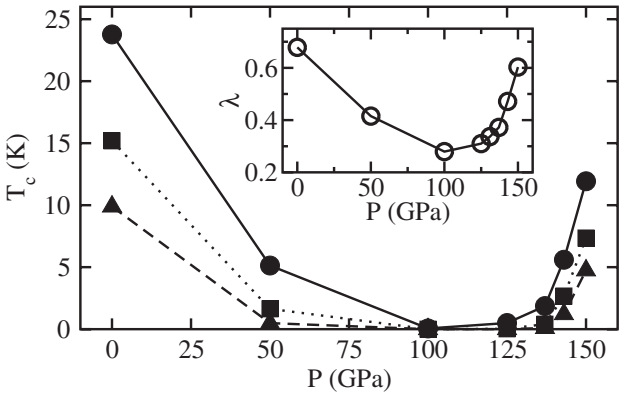

FIG. 6. The calculated superconducting transition temperature T_c in MgB_2 as a function of pressure P for μ^* equal to 0.1 (solid circles connected with solid line), 0.15 (solid squares connected with dotted line), and 0.2 (solid triangles connected with dashed line), respectively. The inset shows the variation of λ with pressure. The λ and T_c at 143 and 150 GPa are obtained by ignoring the coupling of imaginary frequencies.

reemergence of superconductivity in MgB_2 at pressures above 100 GPa. In particular, we find that at 137 GPa MgB_2 will superconduct with $T_c \approx 2$ K for $\mu^* = 0.1$. Because the electron-phonon interaction in MgB_2 at zero pressure is known to be very anisotropic, an accurate determination of T_c requires the solution of the anisotropic gap equation. However, we have seen that the B $p_{x(y)}$-dependent electron-phonon coupling decreases dramatically with increasing pressure, making the use of isotropic gap equation for the calculation of T_c more reliable at higher pressures.

In conclusion, we have studied the effects of pressure on the electron-phonon interaction in MgB_2 using density-functional-based methods. The increase in pressure hardens the lattice and dramatically reduces the contribution of the E_{2g} phonon mode to the electron-phonon coupling. As a result, the superconductivity in MgB_2 vanishes by 100 GPa, only to *reappear* at higher pressures. In particular, we find a superconducting transition temperature $T_c \approx 2$ K for $\mu^* = 0.1$ at a pressure of 137 GPa.

*Electronic address: ppsingh@phy.iitb.ac.in

[1] J. Nagamatsu, N. Nakagawa, T. Muranaka, Y. Zenitani, and J. Akimitsu, Nature (London) **410**, 63 (2001).
[2] J. M. An and W. E. Pickett, Phys. Rev. Lett. **86**, 4366 (2001).
[3] J. Kortus, I. I. Mazin, K. D. Belashchenko, V. P. Antropov, and L. L. Boyer, Phys. Rev. Lett. **86**, 4656 (2001).
[4] P. P. Singh, Phys. Rev. Lett. **87**, 087004 (2001).
[5] K.-P. Bohnen, R. Heid, and B. Renker, Phys. Rev. Lett. **86**, 5771 (2001).
[6] Y. Kong, O. V. Dolgov, O. Jepsen, and O. K. Andersen, Phys. Rev. B **64**, 020501(R) (2001).
[7] H. J. Choi, D. Roundy, H. Sun, M. L. Cohen, and S. G. Louie, Nature (London) **418**, 758 (2002).
[8] T. Yildirim, O. Gulseren, J. W. Lynn, C. M. Brown, T. J. Udovic, Q. Huang, N. Rogado, K. A. Regan, M. A. Hayward, and J. S. Slusky *et al.*, Phys. Rev. Lett. **87**, 037001 (2001).
[9] M. Monteverde, M. Nunez-Regueiro, N. Rogado, K. A. Regan, M. A. Hayward, T. He, S. M. Loureiro, and R. J. Cava, Science **292**, 75 (2001).
[10] T. Tomita, J. J. Hamlin, J. S. Schilling, D. G. Hinks, and J. D. Jorgensen, Phys. Rev. B **64**, 092505 (2001).
[11] S. Deemyaad, T. Tomita, J. J. Hamlin, B. R. Beckett, J. S. Schilling, D. G. Hinks, J. D. Jorgensen, S. Lee, and S. Tajima, Physica (Amsterdam) **385C**, 105 (2003).
[12] Y. Shao and X. Zhang, J. Phys. Condens. Matter **16**, 1103 (2004).
[13] K. Shimizu, H. Kimura, D. Takao, and K. Amaya, Nature (London) **419**, 597 (2002).
[14] V. V. Struzhkin, M. I. Eremets, W. Gan, H.-K. Mao, and R. J. Hemely, Science **298**, 1213 (2002).
[15] J. J. Hamlin, V. G. Tissen, and J. S. Schilling, Phys. Rev. B **73**, 094522 (2006).
[16] C. Probst and J. Wittig, in *Handbook on the Physics and Chemistry of Rare Earths*, edited by J. K. A. Gschneidner and L. Eyring (North-Holland, Amsterdam, 1978), p. 749.
[17] S. Y. Savrasov, Phys. Rev. B **54**, 16 470 (1996).
[18] S. Y. Savrasov and D. Y. Savrasov, Phys. Rev. B **54**, 16 487 (1996).
[19] Plane-wave self-consistent-field code: http://www.pwscf.org/
[20] S. Baroni, S. de Gironcoli, A. D. Corso, and P. Giannozzi, Rev. Mod. Phys. **73**, 515 (2001).
[21] P. B. Allen and R. C. Dynes, Phys. Rev. B **12**, 905 (1975).
[22] P. Allen and B. Mitrovic, in *Advances in Solid State Physics*, edited by H. Ehrenreich, F. Seitz, and E. Turnbull (Academic Press, New York, 1982), Vol. 37, p. 1.
[23] P. B. Allen (private communication).
[24] J. P. Perdew and Y. Wang, Phys. Rev. B **45**, 13 244 (1992).